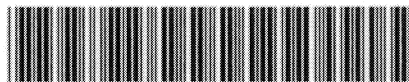


3

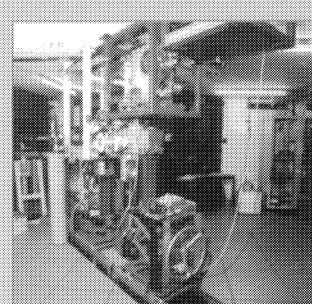
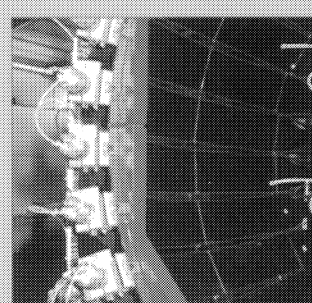
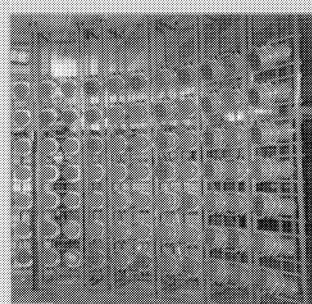
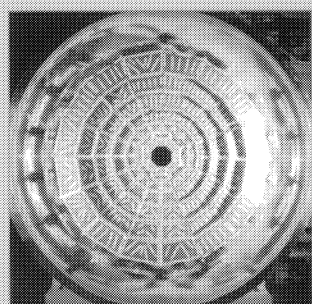


LABORATOIRE DE PHYSIQUE CORPUSCULAIRE

CERN LIBRARIES, GENEVA



CM-P00048385



Evaluation of the power density deposited in
the spallation target of the TRADE experiment

V. Blideanu and J-C. Steckmeyer

LPC/ENSI CAEN, Boulevard du Maréchal Juin, F 14050 Caen Cedex, France

December 2003

LPC C 03-15

CENTRE NATIONAL DE LA RECHERCHE SCIENTIFIQUE
INSTITUT NATIONAL
DE PHYSIQUE NUCLÉAIRE ET DE PHYSIQUE DES PARTICULES
INSTITUT DES SCIENCES DE LA MATIÈRE ET DU RAYONNEMENT
UNIVERSITÉ DE CAEN

U.M.R. 6534
ISMRA 6, Boulevard Maréchal Juin 14050 CAEN CEDEX FRANCE

Téléphone : 02 31 45 25 00 Télécopie : 02 31 45 25 49
Internet : <http://caeinfo.in2p3.fr>



Evaluation of the power density deposited in the spallation target of the TRADE experiment

Valentin Blideanu and Jean-Claude Steckmeyer

Laboratoire de Physique Corpusculaire - ENSICAEN
6 boulevard du Maréchal Juin
14050 CAEN Cedex - France

September 15, 2003

Contents

1	Introduction	2
2	Data	2
2.1	Target	2
2.2	Beam profile	2
2.3	Calculations	3
3	Results obtained with the narrow beam profile	3
3.1	Power density distribution	3
3.2	Power distribution	4
4	Results obtained with the wide beam profile	6
4.1	Power density distribution	6
4.2	Power distribution	7
5	Conclusions	8

1 Introduction

The design of the spallation target of the TRADE experiment [1] requires a precise knowledge of the power density distribution deposited inside the target. Such data are of key importance for thermo-mechanical calculations aiming to determine the stress suffered by the target material. For several reasons (security, licensing, ...) the target material should be able to release the heat deposited by the proton beam in a safe way while keeping its integrity all along the experiment.

2 Data

2.1 Target

The target has a cylinder shape with a total height of 40 cm and a diameter of 3.8 cm. A conic hole is dug into the solid cylinder starting at 3 cm from the bottom of the target. The half-opening angle is 2.25 degrees leading to an aperture with a diameter of 2.91 cm at the top of the target. This geometry will be called the "sharp cone geometry" all along this work.

A second geometry has also been studied: a conic hole starting at 3 cm from the bottom of the target with a spherical shape at the tip with a radius of 1 mm. This configuration will be called the "rounded cone tip geometry".

Wolfram has been fixed as the target material (16.65 g cm⁻³ of density).

2.2 Beam profile

Gaussian beam profiles have been used in the calculations, with a full width at half maximum (FWHM) of 1.32 cm and 1.95 cm, respectively. The second gaussian profile was set to compare with earlier calculations [2] in which a parabolic beam profile was used with an outer beam diameter of 2.64 cm. The two gaussian beam profiles are compared to the parabolic one in Fig. 1.¹

¹The beam profile currently defined by the beam line responsible should deposit 95% of its power in the target. This leads to a full width at half maximum of 1.62 cm, assuming an inner diameter of 2.7 cm. So the actual beam profile is in between the two gaussian beam profiles studied in this work.

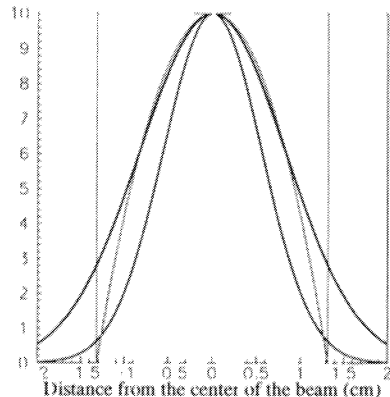


Figure 1 Gaussian beam profiles used in the calculations, the narrower one in red, the larger one in blue. They are compared to the parabolic profile (in green)

2.3 Calculations

The calculations have been performed with the MCNPX code (version 2.2.6) [3]. $10 \cdot 10^6$ proton trajectories were followed for calculations using the narrower beam profile and $2 \cdot 10^6$ trajectories for the wider one. The size of the mesh is 1 mm both in radial (R coordinate) and axial (Z coordinate) directions, except in the cone tip region for which a smaller mesh of 2 mm was used in the two directions. The cone tip region is so defined: $R < 4$ cm and 2 cm $< Z < 6$ cm.

The beam power is 40 kW for a proton beam with an intensity of 286 mA and an energy of 140 MeV.

3 Results obtained with the narrow beam profile

3.1 Power density distribution

In Fig. 2 is displayed the power density deposited in the cone tip region for the two geometries. A maximum value of 21.9 kW cm⁻³ is reached on the symmetry axis at an axial distance 3.42 cm $< Z < 3.44$ cm for the sharp cone geometry, while a slighter value of 20.6 kW cm⁻³ is reached for the rounded

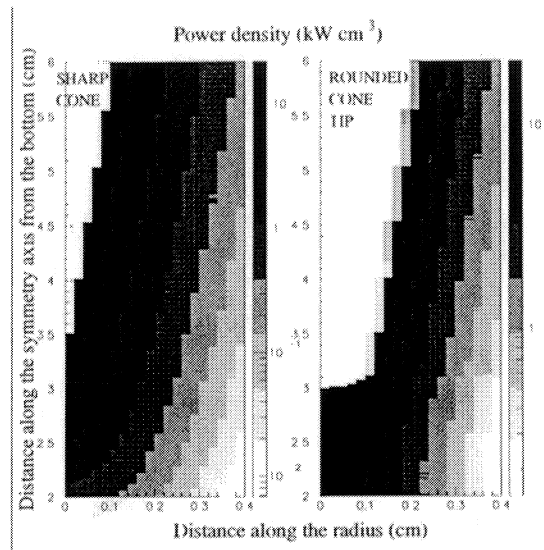


Figure 2 Power density distribution in kW cm^{-3} shown as a function of the axial (vertical) and radial (horizontal) distances for the two geometries, in the cone tip region $R < 4 \text{ cm}$ and $2 \text{ cm} < Z < 6 \text{ cm}$

cone tip geometry at the same axial distance but no more on the symmetry axis it is now located at a radial distance $1.2 \text{ cm} < R < 1.4 \text{ cm}$

3.2 Power distribution

In Fig. 3 are compared the power distributions for the two geometries. In Fig. 4 are shown the same distributions in the cone tip region with a smaller meshing. With the mesh of $1\text{mm} \times 1\text{mm}$, the maximum values of the power are 119.2 W and 119.4 W , respectively, at the same radial distance $4 \text{ cm} < R < 5 \text{ cm}$ but at a different axial distance $13.2 \text{ cm} < Z < 13.3 \text{ cm}$ for the sharp cone geometry and $10.6 \text{ cm} < Z < 10.7 \text{ cm}$ for the rounded cone tip one.

The integrated power distributions are given in Fig. 5: integration over the axial direction (top) and the radial direction (bottom), the sharp cone geometry being represented by the solid line and the rounded cone tip one by the dashed line. As seen in the top of Fig. 5, more power (given by the curve integration) is collected in the latter geometry than in the former one, 38.35 kW compared to 37.51 kW .

In the bottom of Fig. 5 is displayed the power distribution as a function of the axial coordinate. There is a strong shift of the power deposit towards the bottom of the target for the rounded cone tip geometry. The structures

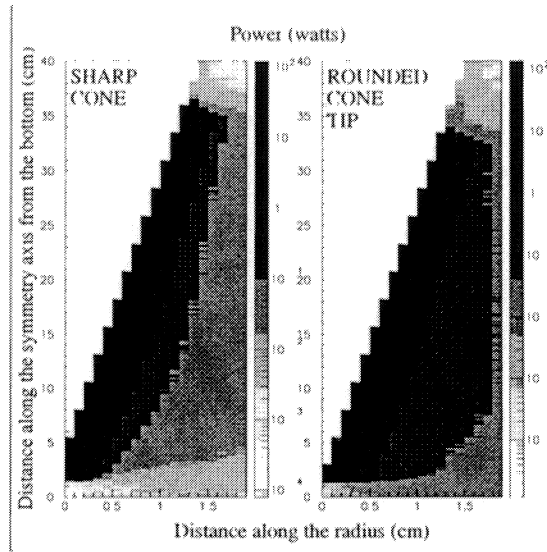


Figure 3 Power distribution in watts shown as a function of the axial (vertical) and radial (horizontal) distances for the two geometries

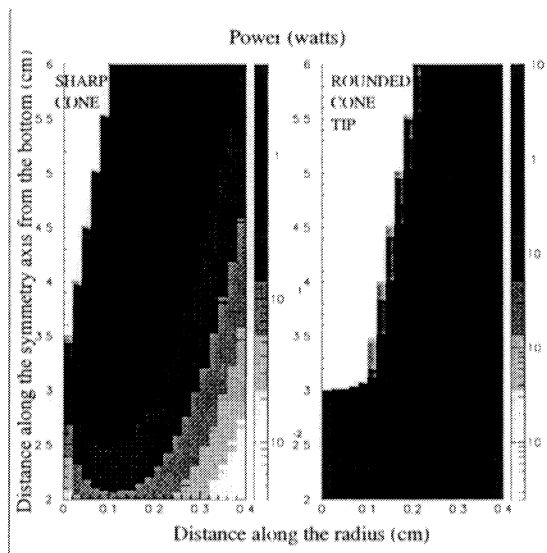


Figure 4 Same as in Fig 3 for the cone tip region $R < 4$ cm and 2 cm $< Z < 6$ cm

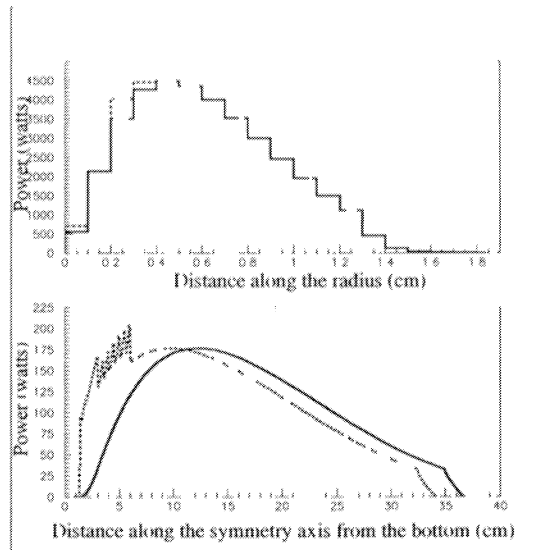


Figure 5: Integrated power distributions (top) integration over the Z axial direction, (bottom) integration over the R radial direction. The sharp cone geometry is represented by the solid line and the rounded cone tip geometry by the dashed line.

observed in the cone tip region result from this specific geometry. By looking at Fig. 2 it is seen that the power density is no more located along the cone side, as it is the case in the sharp cone geometry, but slightly inside the target material.

From Fig. 5 it is seen that power cannot escape from the target in the radial direction ($R > 1.9$ cm) neither from the bottom of the target ($Z < 0$ cm). The loss of power is likely associated with protons backscattered in the vacuum pipe.

4 Results obtained with the wide beam profile

4.1 Power density distribution

Results obtained with a wider beam profile are shown in Fig. 6. They have to be compared with those of Fig. 2. No significant difference appears. The only change concerns the maximum values of the power density deposit.

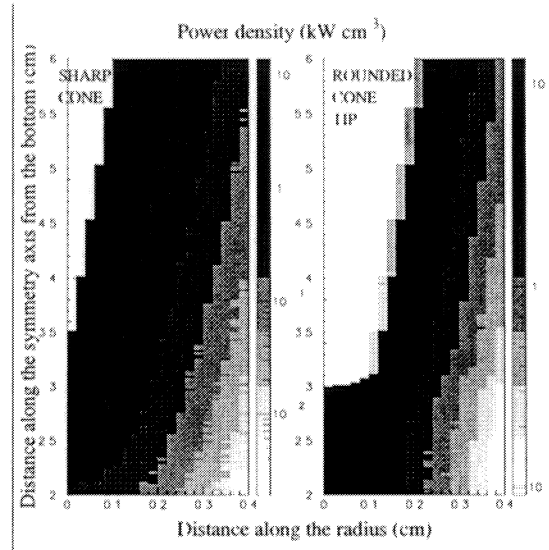


Figure 6 Same as Fig. 2 with a wider gaussian beam profile (FWHM of 1.95 cm instead of 1.32 cm)

They are much smaller than those calculated using a narrow beam profile 13.9 kW cm^{-3} for the sharp cone geometry and 13.4 kW cm^{-3} for the other one. The location of these maximum values is on the symmetry axis at an axial distance $3.46 \text{ cm} < Z < 3.48 \text{ cm}$ in the first case and $2.58 \text{ cm} < Z < 2.60 \text{ cm}$ in the second one.

4.2 Power distribution

As for the power density, the maximum values of the power are reduced 100.6 W and 100 W , respectively, located at the same axial distance $15.7 \text{ cm} < Z < 15.8 \text{ cm}$ and at a radial distance $4 \text{ cm} < R < 5 \text{ cm}$ for the sharp cone geometry and $5 \text{ cm} < R < 6 \text{ cm}$ for the rounded cone tip geometry.

The integrated power distributions displayed in Fig. 7 can be compared to those of Fig. 5. With a wider beam profile, the power distributions become broader and more symmetrical. The maximum power deposit location is shifted towards larger axial and radial distances.

Again, as observed with the narrow beam profile, the power collected in the sharp cone geometry is slightly smaller than the one collected with the rounded cone tip geometry 37.49 kW versus 38.04 kW . As expected, these values are also slightly weaker than those calculated with the narrow beam profile.

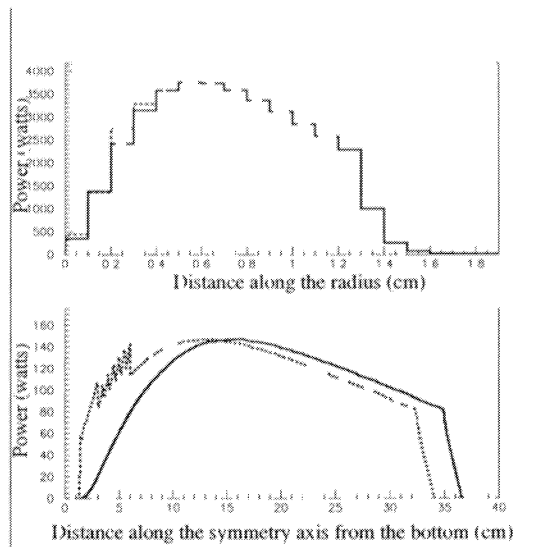


Figure 7: Integrated power distributions (top) integration over the Z axial direction, (bottom) integration over the R radial direction. The sharp cone geometry is represented by the solid line and the rounded cone tip geometry by the dashed line.

5 Conclusions

For a given beam profile, similar maximum values of the power density and of the power are reached, whatever the considered geometry. The maximum of the power density is shifted towards lower values in axial and radial directions when going from the sharp cone geometry to the rounded cone type one. More power is collected with the latter configuration as the beam penetration is deeper.

For a given geometry, the maximum value of the power density is decreased by one third and the maximum power by one fourth when going from a narrow beam profile to a wider one. The integrated power distributions are broader and more symmetrical. The power is better shared out.

In all cases, a fraction of the incident power of the proton beam is lost: this amounts to 5.6% and is mainly associated with protons backscattered when interacting with the target material.

References

- [1] TRADE Final Feasibility Report - March 2002
- [2] Y Kadi, 7th TRADE General Progress Meeting, Roma, April 16, 2003
- [3] L S Waters, Ed , MCNPX User's Manual, Version 2 2 0